2002 International Radon Symposium Proceedings

Relationship Between the Permeability Coefficient of Concrete and Low-Pressure Differentials

Esam Abu-Irshaid and Kevin J. Renken
University of Wisconsin-Milwaukee
Mechanical Engineering Department
Radon Reduction Technology Laboratory
3200 North Cramer Street
Milwaukee, Wisconsin 53211
USA

ABSTRACT

This paper presents experimental results on the permeability coefficient of concrete under low-pressure differentials. Three concrete samples have been exposed to differential pressures ranging between 1 Pa and 1 psi under controlled conditions. The laboratory tests simulate indoor radon gas entry by advection ($\Delta p \sim 1 - 20$ Pa). The permeability coefficient is measured by a unique control system that employs sensitive pressure transducers, needle control valves, thermistors, and relative humidity sensors connected to a sophisticated PC-data acquisition and control system. The concrete samples are 4" in length and 3.5" in diameter and are maintained in aluminum holders. The concrete mixtures are standard compositions that simulate typical Wisconsin concretes used in basement foundations. The experimental results highlight the *slip effect* that produces higher values of the permeability coefficient at very low-pressure differences. Details of the innovative experimental setup and procedures are described.

INTRODUCTION

Calculations on the indoor radon entry rate by pressure-driven flow rely on the permeability coefficient of the concrete. The permeability coefficient is the transport coefficient for permeability, and is the proportionality constant in Darcy's law that relates fluid flux through a porous material (e.g., concrete) to the pressure gradient. In typical radon problems, the pressure difference across the foundation walls may range between 1 – 20 Pa. However, there exists very little experimental data on the permeability coefficient of air in concrete for these low-pressure differences. The majority of studies have documented permeability coefficients at differential pressures beyond the scope of advective radon entry problems in residential construction (Nielson and Rogers 1991; Rogers and Nielson 1992; Snoddy 1994). Permeability measurements under specified high pressure difference conditions have been found not to scale linearly to the small pressure differences of interest. This nonlinearity for large pressure differences normally leads to an underestimate of the flow velocity at low-pressure difference conditions and hence, a large variance in the permeability value (Colle 1981). These previous experimental investigations have neglected to account for the *slip effect* (or limitations of Darcy's law) found at low pressures when extrapolating values of K. If permeability measurements are made under conditions different from those for which they are to be applied, a correction factor has to be made. This correction is represented by the *slip effect* where the superficial gas permeability (i.e., the value of K in Darcy's law) is a linear function of the inverse mean pressure of the gas. Since the cause of this dependence is gas slippage, it increases with increasing free path length (Sheidegger 1974).

To characterize this limitation in Darcy's law, an innovative laboratory apparatus to accurately measure the concrete air permeability at low-pressure differences that simulate indoor radon gas entry by advection was introduced by Abraham et al. (2000). This study also compared permeability coefficients for several experimental investigations that used pressure differences in the order of magnitude of one psi. Ferguson et al. (2001) continued this research by reporting preliminary experimental data on the permeability coefficient of concrete subjected to constant pressure differences between 5 – 15 Pa.

This paper is a continuation of the work presented by Ferguson et al. (2001). Utilizing the same automated permeability apparatus fabricated by Abraham et al. (2000), the authors measure the permeability coefficient of three concrete samples of different formulas over a wide range of applied pressure differences (1 Pa – 1 psi). Measurements at very low differential pressures ($\Delta p \sim 1 - 20$ Pa) simulate indoor radon entry by advection and highlight the *slip effect*.

PERMEABILITY COEFFICIENT

The permeability coefficient (K) is the proportionality constant in Darcy's law that relates the fluid flux through a porous material (e.g., intact concrete) to the pressure gradient. The value of K dictates the indoor radon entry rate by the advection transport mechanism. Darcy's law as applied to our experimental setup is expressed as:

$$Q = -\frac{KA\Delta p}{\mu L} \qquad (1)$$

where,

- Q = volumetric flow rate of air
- K = permeability coefficient
- A = cross-sectional area of the concrete sample
- Δp = applied pressure difference across the concrete
- μ = viscosity of air
- L = thickness of concrete sample.

The volumetric flow rate of air through the concrete pores is calculated from the ideal gas law and the molecular volume of air as described by Maas and Renken (1997).

CONCRETE SAMPLES

Table 1 provides a description of the concrete test samples used in this study. The three concrete samples simulate standard Wisconsin poured-concrete for basement foundations (Hool 1918; USBR 1938). The ingredients for the concrete samples were cement, sand, stones, and water. Pea gravel was used to obtain a

homogeneous mixture with respect to the sample size. A water-to-cement ratio (w/c) of 0.5 was used and the ratio of the concrete ingredients (cement:sand:pea gravel) was 1:2:4 (Sample A) and 1:2:2 (Samples B1 and B2). As shown in Figs. 1 and 2, a cylindrical aluminum casing was employed to cast and hold the concrete samples for testing. As per ASTM specifications (ASTM 1994), the concretes were removed from the holders 24 hours after casting and placed in a high humidity chamber for 30 days. After curing, the samples were allowed to dry at ambient conditions for one week. The samples were then placed back into the cylindrical holders and the circumferences of each were sealed with a cementitious epoxy.

The porosity (ε) of each concrete sample was measured by using a concrete porosity measurement system first introduced by Maas and Renken (1997). Figure 3 displays a schematic diagram of this porosity apparatus. As expected, Sample A has a porosity that is approximately 31% larger than Samples B1 and B2. The porosities of Samples B1 and B2 differ by approximately 7%. The experimental uncertainty of these measurements is $\pm$ 3%.

PERMEABILITY APPARATUS

As shown in Figs. 4 and 5, the same permeability apparatus used by Ferguson et al. (2001) is employed in this study. More specifically, the system consists of a clean air pressure source, two pressure chambers (high and low), the concrete samples situated between the chambers, two miniature proportional flow control valves, pressure transducers, thermistors, humidity sensors, and a high-speed PC-data acquisition and control system (PC-DACS). An accompanying commercial programming language is employed to monitor pressure conditions and to electronically control the operation of the needle control valves. Figure 6 presents a detailed schematic diagram of the permeability measurement system. Complete details of the automated operation of the system are described in Abraham et al. (2000).

DISCUSSION OF RESULTS

Figure 7 displays the experimental data generated by this study. More specifically, Fig. 7 presents a comparison of the measured air permeability coefficients for Samples A, B1, and B2. The differential pressure applied to the concrete samples during testing ranged between 1 Pa and 1 psi (6,895 Pa). As shown, there exists a logarithmic increase in the value of K for all three samples as the applied pressure difference is decreased. An approximate 100,000% increase in the average value of K is realized for all samples when Δp is decreased from 1 psi to 1 Pa. As the applied pressure difference increases beyond 10^3, we start to see a leveling-off effect of the permeability coefficients. Here, there exists an approximate 10% difference in the value of K between 5,000 Pa and 1 psi (6,895 Pa) for all three concrete samples.

These experimental findings verify and complement the hypotheses of Abraham et al. (2000) and Ferguson et al. (2001). These studies suggested significant increases in the permeability coefficient at very low differential pressures could be attributed to the *slip effect*. Permeability measurements at high-pressure differences (e.g., 1 – 100 psi) have been found not to scale linearly to small pressure differences (e.g., 1 – 20 Pa) symbolic of advective or pressure-driven radon entry problems (Colle 1981; Abraham et al. 2000, Ferguson et al. 2001). Therefore, the authors conclude that Darcy's law needs to be modified with a *slip effect* coefficient for very low-pressure differences across concretes. Previously published data on permeability measurements under

specified high-pressure differences have underestimated the flow for low-pressure calculations by neglecting a correction factor for slip. This has resulted in a significant underestimation of indoor radon entry rates (Ferguson et al. 2001).

To better illustrate this underestimation of radon entry rate prediction, we can use the simple model of Nazaroff and Nero (1988) to approximate indoor radon concentrations due to advective flow between radon-laden soil and a typical detached house. Here, the radon gas entry rate per unit volume for a 1 Pa pressure difference across a typical intact concrete basement wall is estimated by Darcy's law (Eqn. 1) where,

$K_{avg.}$ = 1.92×10^{-16} m^2 (based on experimental data at 1 psi for Sample A)
A = 140 m^2 (typical foundation wall surface area)
Δp = 1 Pa (pressure difference across a foundation wall)
μ = 1.846×10^{-5} kg/m-sec (viscosity of air at room temperature)
L = 0.10 m (4" thick concrete foundation wall).

If we assume an average radon concentration in the soil of 2,700 pCi/L (Nagda 1994), a house volume of 10^3 m^3, and a house ventilation rate of 0.25 ACH, we find the indoor equilibrium radon concentration level due to advective entry through the concrete foundation wall is approximately I = 0.39 pCi/L. Now, using the same parameters and the value of K measured at 1 Pa for Sample A, we find the indoor equilibrium radon concentration to be approximately I = 0.94 pCi/L. A 141% increase in the indoor radon level is realized. If we use a very tight house in the calculation (~ 0 ACH), the results are even more significant. This calculation yields indoor equilibrium radon concentrations of I = 0.011 and 18.6 pCi/L when the permeability coefficient is based on experimental data at 1 psi and 1 Pa, respectively.

Figure 7 also displays the effect of concrete ingredients on the value of the permeability coefficient at low applied differential pressures. Here, we see the overall permeability of Sample A is greater than Samples B1 and B2 over the entire Δp test range. This is attributed to the higher porosity of Sample A. Concretes with more pore volume are more likely to allow greater flow rate, hence greater permeability. Renken and Rosenberg (1995) and Lambert and Renken (1999) found similar trends in the permeability coefficient for higher porosity concretes.

Finally, Fig. 7 provides a comparison of the permeability coefficient between two nearly identical concrete samples, B1 and B2. Samples B1 and B2 were fabricated at the same time with the same batch of concrete mix. As expected, there exists a very tight overlap in measured values of K over the entire range of applied Δp. This data verifies the experimental method used to determine the relationship between the permeability coefficient and the applied pressure difference. Table 2 provides the empirical relationships between K and Δp for the three test samples. The experimental uncertainty of the measured permeability coefficient is $\pm$5% (Abraham et al. 2000).

CONCLUSIONS AND RECOMMENDATIONS

This paper presented empirical correlations of the permeability coefficient of concrete versus applied pressure differences. Three concrete samples of two different formulas were exposed to pressure differences in the range

of 1 Pa – 1 psi. It was found that there exists a significant difference in the permeability coefficient when the pressure differential across the concrete approaches *real* indoor radon entry conditions ($\Delta p \sim 1 - 20$ Pa). When the applied pressure difference approaches 1 psi, there is minimal difference in the value of the permeability coefficient. This significant difference in the permeability is attributed to the *slip effect* and is highlighted when applied to the estimation of indoor radon entry rates by advection. It is recommended that further tests be conducted to fully characterize a *slip effect* coefficient and its dependence on applied pressure difference, concrete composition and age, and relative humidity level.

ACKNOWLEDGEMENTS

The authors would like to thank Ms. Kimberly Jonet and Ms. Laura Ferguson for their initial work on this project. Special thanks to Mr. George T. Abraham for his ideas and fabrication of the original control loop system.

REFERENCES

Abraham, G. T.; Daoud, W. Z.; Renken, K. J. Experimental measurements on the permeability coefficient of a concrete sample under low pressure differences. In: The 2000 International Radon Symposium Pre-Prints. 12.1 – 12.12 Milwaukee, WI: AARST; 2000.

American Society for Testing Materials (ASTM). Standard practice for making and curing concrete test specimens in the laboratory. Annual Book of ASTM Standards. Designation C 192 - 90a; 1994.

Colle, R; Rubin, R. J.; Knab, L. I.; Hutchinson, J. M. R. Radon transport through and exhalation from building materials: a review and assessment. National Bureau of Standards, Technical Note 1139. Washington, DC; 1981.

Ferguson, L. J.; Daoud, W. Z.; Renken, K. J. Further measurements on the permeability coefficient of a concrete sample under low pressure differences. In: The 2001 International Radon Symposium Pre-Prints. 78 – 86 Daytona Beach, Florida: AARST; 2001.

Hool, G. A. Concrete Engineer's Handbook. New York: McGraw-Hill; 1918.

Lambert, T. L.; Renken, K. J. Experiments on industrial by-product utilization as a concrete admixture to reduce radon gas transport properties. In: The 1999 International Radon Symposium Pre-prints. 13.0-13.10 Las Vegas, NV: AARST; 1999.

Maas, J .J.; Renken, K. J. Laboratory assessment of cementitious coatings as a barrier to radon gas entry. In: The 1997 International Radon Symposium Pre-Prints. 1.1 - 1.13 Cincinnati, OH: AARST; 1997.

Nagda, N. L. Radon: prevalence, measurements, health risks and control. ASTM Manual Series, Philadelphia, PA: ASTM; 1994.

Nazaroff, W. W.; Nero, A. V. Radon and its decay products in indoor air. New York: John Wiley & Son; 1988.

Nielson, K.K.; Rogers, V.C. Radon entry into dwellings through concrete floors. In: The 1991 International Symposium on Radon and Radon Reduction Technology. Vol. 3: US EPA; 1991.

Renken, K. J.; Rosenberg, T. Laboratory measurements of the transport of radon gas through concrete samples. Health Physics. 68:800-808; June 1995.

Rogers, V.C.; Nielson, K.K. Data and models for radon transport through concrete. In: The 1992 International Symposium on Radon and Radon Reduction Technology. Vol. 3: US EPA; 1992.

Sheidegger, A.E. The Physics of Flow Through Porous Media. Toronto, Canada: University of Toronto Press; 1974.

Snoddy, R. Laboratory assessment of the permeability and diffusion characteristics of Florida concretes, phase I, methods development and testing. EPA-600/R-94-053. US EPA, Research Triangle Park, NC; April 1994.

United States Bureau of Reclamation (USBR). Concrete manual: a manual for the control of concrete construction. Denver, CO: USBR; 1938.

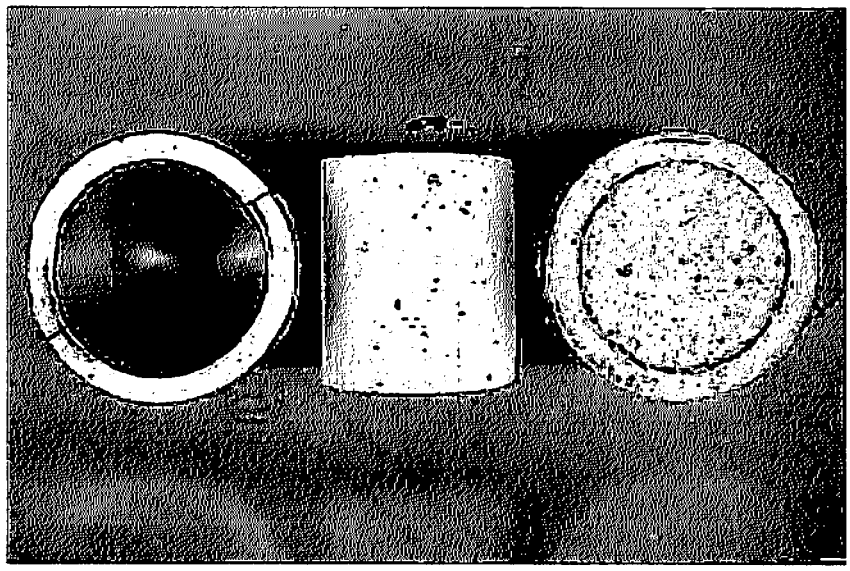

Fig. 1. Photo of concrete sample in an aluminum holder.

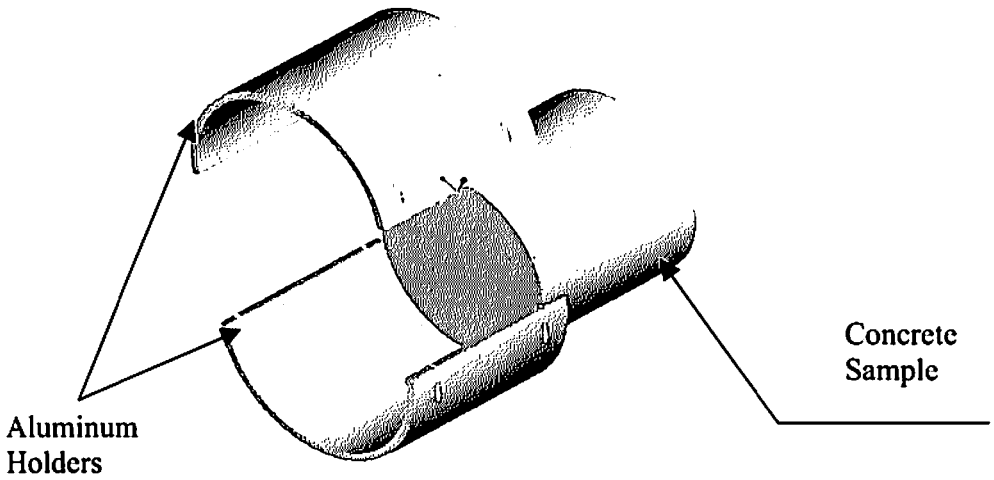

Fig. 2. Schematic of concrete sample and aluminum holder.

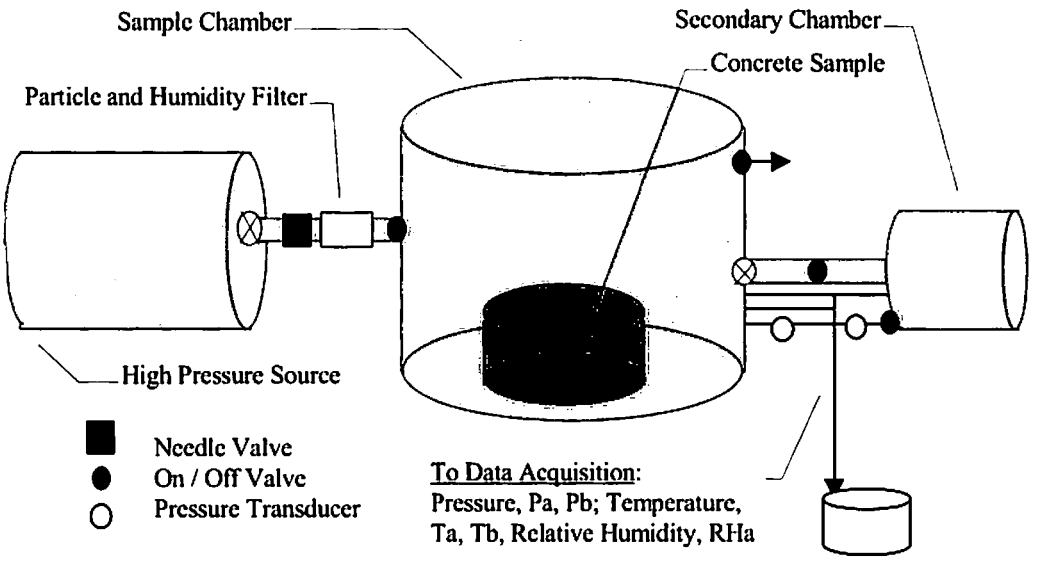

Fig. 3. Schematic diagram of porosity apparatus (Maas and Renken 1997).

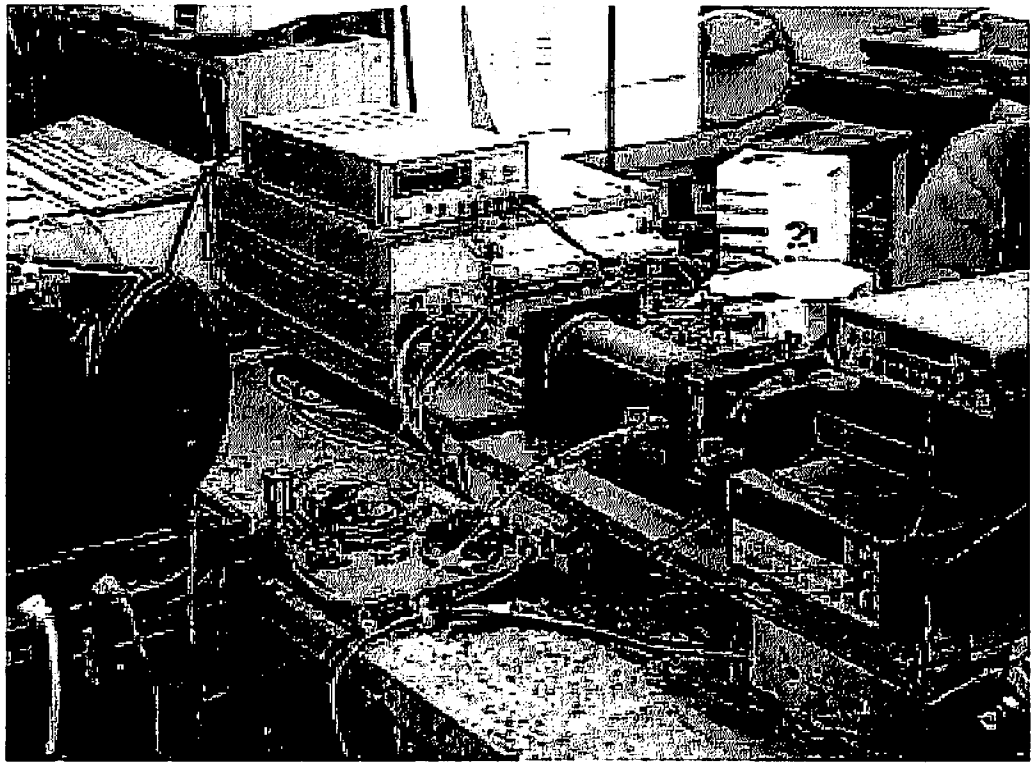

Fig. 4. Photo of experimental apparatus to measure the air permeability of concrete.

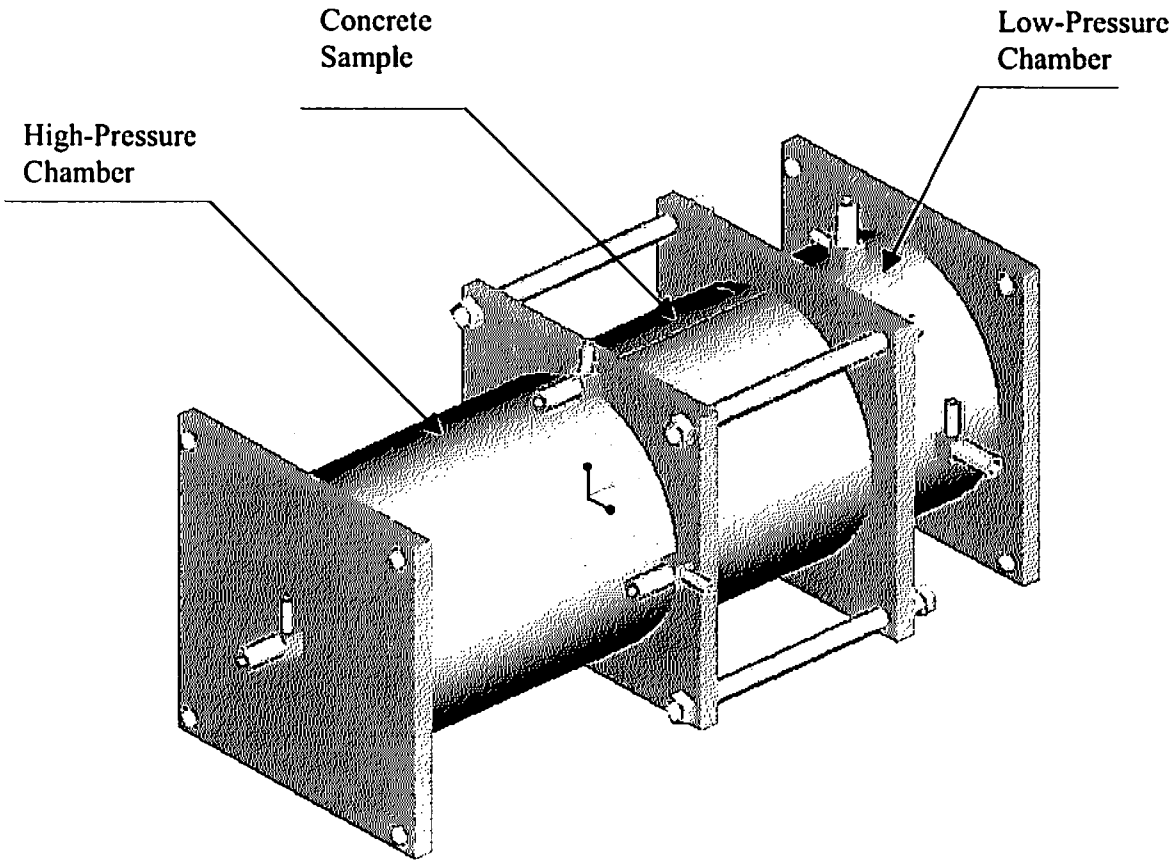

Fig. 5. Schematic of permeability apparatus.

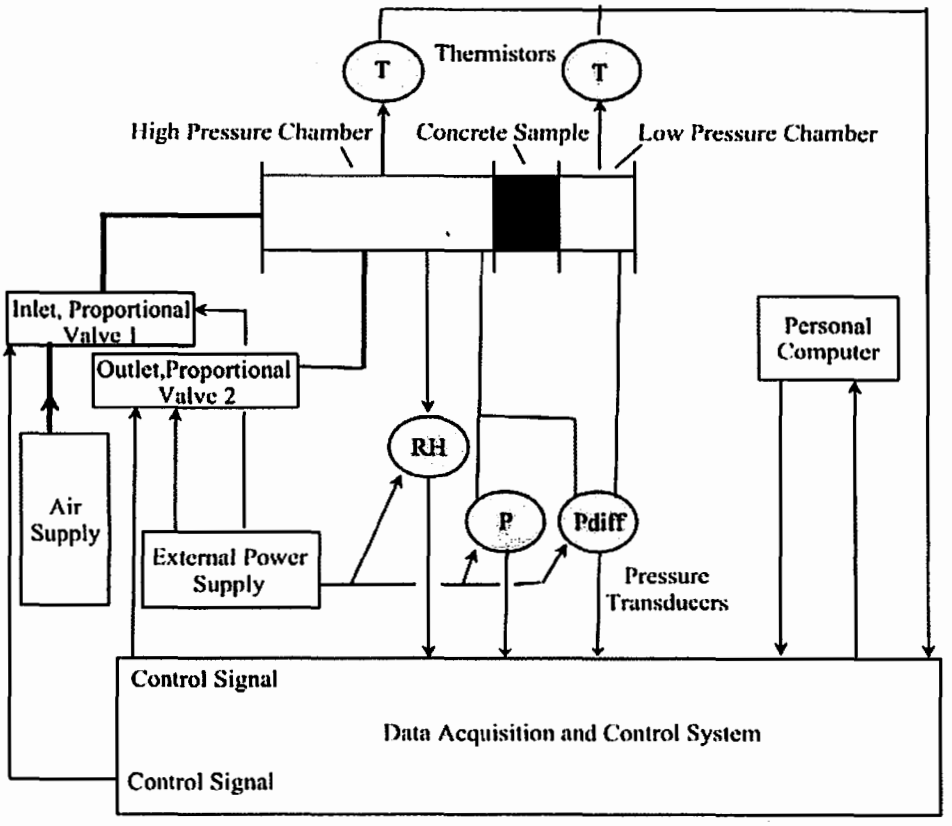

Fig. 6. Schematic diagram of system to measure the air permeability coefficient of concrete.

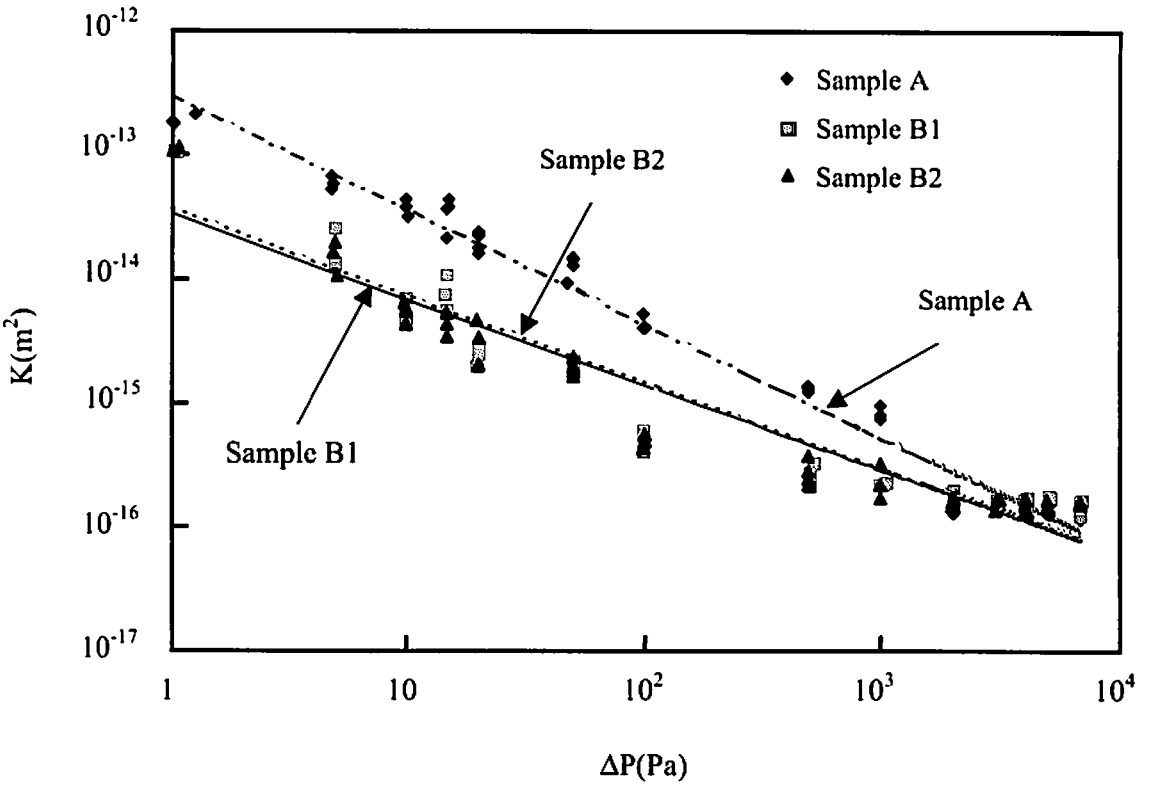

Fig.7. Measured air permeability coefficients for Samples A, B1, and B2.

Table 1. Description of concrete test samples.

Sample	Cement:Sand:Pea Gravel	w/c	D (in.)	L (in.)	Porosity, ε (%)
A	1:2:4	0.5	3.5	4	18.8
B1	1:2:2	0.5	3.5	4	14.9
B2	1:2:2	0.5	3.5	4	13.8

Table 2. Empirical relationships between permeability coefficient and applied pressure difference for concrete test samples.

Sample	K vs. Δp
A	$K = 3.0 \times 10^{-13} \Delta p^{-0.918}$
B1	$K = 4.0 \times 10^{-14} \Delta p^{-0.693}$
B2	$K = 3.0 \times 10^{-14} \Delta p^{-0.688}$